Structural Dynamics of the *Streptomyces lividans* K^+ Channel (SKC1): Oligomeric Stoichiometry and Stability[†,‡]

D. Marien Cortes and Eduardo Perozo*

Department of Molecular Physiology and Biological Physics, University of Virginia Health Sciences Center, Charlottesville, Virginia 22906-0011

Received May 1, 1997; Revised Manuscript Received June 13, 1997[⊗]

ABSTRACT: SKC1, a 160-residue potassium channel with two putative transmembrane (TM) segments was recently identified from *Streptomyces lividans*. Its high levels of expression, small size, and ease of purification make SKC1 an ideal candidate for high-resolution structural studies. We have initiated the structural characterization of this channel by assessing its oligomeric behavior, stability in detergent, general hydrodynamic properties, and preliminary secondary structure content. SKC1 was readily expressed and purified to homogeneity by sequential metal-chelate and gel filtration chromatography. Standard SDS−PAGE, together with chemical cross-linking analysis indicated that SKC1 behaves as a tightly associated tetramer even in the presence of SDS. Using a gel shift assay to assess its oligomeric state, we determined that SKC1 is stable as a tetramer in most detergents and can be maintained in nonionic detergent solutions for extended periods of time. The tetramer is also stable at relatively high temperatures, with an oligomer-to-monomer transition occurring at approximately 65 °C. The Stokes radius of the micellar complex is 5 nm as determined from gel filtration chromatography of SKC1 in dodecyl maltoside. Preliminary estimations of secondary structure from CD spectroscopy showed that the channel exists mostly in α-helical conformation, with more than 50% α-helical, close to 20% β-sheet, 10% β-turn, and about 15% unassigned or random coil. These results are consistent with the idea that a bundle of α-helices forming a tetramer around the ion-conductive pathway is the common structural motif for members of the voltage-dependent channel superfamily.

Potassium-selective channels are ubiquitous membrane proteins that play a key role in cells as regulators of electrical activity, osmotic balance, signal transduction, and many other physiological events. The application of molecular biology and related technologies to the study of ion channels has produced a wealth of primary sequence information suggesting that K^+ channels belong to a voltage-dependent superfamily of channels (*1*). This superfamily includes Na^+ and Ca^{2+} channels as well as other K^+ channels not intrinsically voltage-dependent (i.e., the inward rectifier family).

As has been suggested by analysis of primary sequences, these types of proteins conform to a common structural motif, involving multiple transmembrane segments arranged as helical bundles (*2*). These bundles form oligomeric structures by the association of subunits (as in K channels) or homologous pseudo-subunits (as in Na^+ and Ca^{2+} channels) around an ion-conductive pathway. Although a great deal of information has been gathered on the voltage-dependent K^+ channel family based on electrical measurements of activity (*3*−*5*), their sheer complexity and lack of adequate protein sources have prevented high-resolution structural studies.

Recently, the cloning of a novel member of the K^+ channel family from the gram-positive bacteria *Streptomyces lividans* was reported (*6*). This channel (SKC1)[1] is a small protein of 160 residues that has two putative transmembrane (TM) segments, a 40 pS K-selective conductance, and little overall similarity to other K^+ channels. However, SKC1 contains a highly conserved pore region that includes the K^+ channel "signature sequence" (*7*), and shows 64% identity with the pore of Shaker. Although the two-TM segment arrangement of SKC1 is reminiscent of inward rectifier channels, sequence similarity analysis of the pore region indicates that this channel is more closely related to voltage-dependent channels (*6*). Schrempf et al. also reported that SKC1 expresses in *Escherichia coli* at milligram levels under fairly standard conditions. This is a remarkable characteristic, considering that previous efforts to overexpress other putative K^+-selective channels from bacteria (*8*) have not been successful.

The high levels of expression, small size, and ease of purification make SKC1 an ideal candidate for high-resolution structural studies. In this report we have started the structural characterization of this channel by assessing its stability in detergent, oligomeric behavior, general

[†]Supported by USPHS Grant GM RO1-54690.

[‡] This paper is dedicated to Dr. Carlo Caputo on occasion of his 60th birthday.

* Corresponding author. Phone: (804) 243-6580. FAX: (804) 982-1616. E-mail: eperozo@virginia.edu.

[⊗] Abstract published in *Advance ACS Abstracts,* August 1, 1997.

[1] Abbreviations: SKC1, small K^+ channel from *Streptomyces lividans*; TM, transmembrane segment; DDM, dodecyl D-Maltoside; Cymal 5, cyclohexylpentyl D-maltoside; OG, octyl D-glucoside; Fos-Choline-10, *n*-decylphosphocholine; Mega 9, nonanoyl-*N*-methylglucamide; Hega10, decanoyl-*N*-hydroxyethylglucamide; C8E4, *n*-octyltetraoxyethylene; DOC, deoxycholate; SDS, lauryl sulfate; CHAPS, 3-[(3-cholamidopropyl)dimethylammonium]-1-propanesulfonate; PCR, polymerase chain reaction; IPTG, isopropyl thiogalactoside; PBS, phosphate-buffered saline; CMC, critical micellar concentration; PVDF, polyvinylidene fluoride; PTS, 1,3,6,8-pyrenetetrasulfonic acid; V_o, column void volume; V_T, total volume; K_{av}, distribution coefficient; V_e, elution volume; DST, disuccinimidyl tartarate; DSG, disuccinimidyl glutarate; DSS, disuccinimidyl suberate; DMA, dimethylapidimate-2HCL; ECL, enhanced chemiluminescence; CD, circular dichroism; [Θ], molar ellipticity; MRW, mean residue weight.

S0006-2960(97)01018-0 CCC: $14.00

hydrodynamic properties, and preliminary secondary structure content.

EXPERIMENTAL PROCEDURES

Materials

S. lividans was purchased from American Type Culture Collection (Rockville, Maryland) as a freeze-dried culture (ATCC No. 69441), and *E. coli* XL-1 Blue was purchased from Stratagene (La Jolla, CA). Dodecyl β-D-maltoside (DDM), Cymal 5, octyl β-D-glucoside (OG), Fos-Choline, Mega 9, and Hega 10 were obtained from Anatrace (Maumee, Ohio). C8E4 was from Bachem (Torrance, CA). SDS, CHAPS, deoxycholate (DOC), and Triton X-100 were purchased from Calbiochem (La Jolla, California), lauryl sarcosine was from Fluka (Neu-Ulm, Switzerland), and Lubrol PX was from Sigma (St. Louis, MO). Anti-RGS-(4 $\times$ His) antibody was from Qiagen (Chatsworth, CA). The cross-linkers disuccinimidyl suberate (DSS), disuccinimidyl glutarate (DSG), disuccinimidyl tartarate (DST), and dimethylapidimate-2HCl (DMA) were from Pierce (Rockford, IL). Horseradish peroxidase-conjugated anti-mouse antibodies and the enhanced chemiluminescence (ECL) reagents were from Amersham (Buckinghamshire, U.K.). Molecular weight standards were from New England Biolabs, and prestained molecular weight markers were obtained from Bio-Rad (Richmond, CA). All other reagents were from Sigma or Fisher Biotech.

PCR Cloning, Expression, and Purification of SKC1

Streptomyces Culture and Genomic DNA Preparation. Spores from *S. lividans* were initially plated in complete-media/agar [for 1 liter: tryptic soy broth (Difco), 30 g; yeast extract (Difco), 10 g; sucrose, 103 g; $MgCl_2$, 10.12 g; and 10 mL of $CaCl_2$, 332 mM], according to Pigac et al. (*9*). A 0.2 mL aliquot of concentrated spore suspension was used to inoculate 500 mL of complete media, which was grown at 30 °C for 48 h with vigorous shaking. The mycelia was harvested in a Buchner filter on two sheets of Whatman filter paper No. 1, washed with 10% glycerol, and stored as a frozen paste at −20 °C. 50 mg amount of mycelium paste was resuspended in 500 μL of lysozyme solution (2 mg/mL lysozyme, 50 μg/mL RNAse in 0.3 M sucrose, 25 mM Tris-OH, 25 mM EDTA, pH 8.0) and subsequently incubated at 37 °C for 30 min. Cells were lysed by addition of 50 μL of 2% SDS and vortexed for 1 min until the viscosity of the solution decreased noticeably. DNA was purified from crude material after mechanical shearing by sonication (*10*).

PCR Cloning. A 0.5 ng amount of *S. lividans* genomic DNA was used as a template for oligonucleotide-directed polymerase chain reaction (PCR). Oligonucleotide primers SKC1-F (20mer, 5′AGTGAAGATCGGTTACGGAC3′) and SKC1-R (19mer, 5′AGATGTCGTAGGTCTTGCG3′) were used for 30 cycles of PCR. The resultant 851 bp product was gel purified and cut with *Sph*I and *Sal*I, and the 549 bp piece was ligated into pQE32 in frame with a polyhistidine sequence contained in the vector. The open reading frame included in this segment was sequenced completely and was found to be identical to the small potassium channel reported by Schrempf et al. (*6*). The final construct added the following amino acid sequence to the N-terminus of SKC1: MRGSHHHHHHGIR, and this sequence has the RGS-(4 $\times$ His) epitope, which was used for immunodetection of expressed SKC1. This construct was used for all experiments reported in this work.

High-Level Expression and Purification of SKC1. *E. coli* XL-1 Blue cells were transformed with the SKC1-pQE32 construct by electroporation using standard methods. The cells were plated on LB-agar plates containing 100 μM ampicillin, and a single colony was picked and grown in suspension overnight. A 50 mL amount of this culture was diluted into 450 mL of LB media containing 100 μM ampicillin and grown at 37 °C to exponential phase. Protein expression was induced by addition of 1 mM isopropyl thiogalactoside (IPTG) for 2 h. Cells were pelleted, washed twice in phosphate-buffered saline (PBS: 137 mM NaCl, 2.7 mM KCl, 4.3 mM Na_2HPO_4, 1.4 mM K_2HPO_4), resuspended in a small volume of PBS + protease inhibitor cocktail (1 mM phenylmethylsulfonyl fluoride, 300 ng/mL leupeptin, 300 ng/mL pepstatin), and treated with 10 μg/mL of egg lysozyme on ice for 1 h. Spheroplasts were obtained from the lysozyme-treated cells by dilution in hypotonic buffer (50 mM K_2HPO_4) according to ref 11. The spheroplast preparation was washed with PBS, and aliquots were stored at −70 °C.

For purification purposes, 3 g of spheroplasts (equivalent to 1 L of original *E. coli* culture) was solubilized in PBS, pH 8.0, containing DDM at 10$\times$ its critical micellar concentration (CMC), for 1 h at room temperature. This mixture was centrifuged for 1 h at 100000*g*, and the supernatant (approximately 25 mL) was combined with 5 mL of a Co^{2+}-based metal-chelate chromatography resin (Talon resin, Clontech, Palo Alto, CA) for 20 min. After washing the resin extensively with 1 mM DDM in PBS, the channel protein was eluted with a 50−500 mM gradient of imidazole. Protein peaks were identified by the Bradford protein assay (*12*). Fractions containing the channel peak were pooled and concentrated approximately 10-fold by ultrafiltration through 30 000 MWC membranes (Filtron, Northborough, MA). Gel filtration chromatography, the final purification step, was performed on a Superdex 200 (Pharmacia Biotech, Uppsala, Sweden) column, and the eluate was monitored from absorbance measurements at 280 nm. Fractions containing the channel were pooled and either used directly or reconstituted into lipid vesicles. Final yield of pure material was 2−4 mg/L of original culture.

Protein Reconstitution. Asolectin (from soybean lipids, type IV-S, Sigma) was initially purified by ether/acetone precipitation (*13*), solubilized as a chloroform stock (20 mg/mL), and stored under nitrogen. For each reconstitution, the chloroform was dried in a rotary evaporator and the sample further incubated in high vacuum overnight. The dried lipid was resuspended in PBS containing 1 mM DDM and used as the lipid source for all reconstitutions. Two methods of reconstitution were used, a dilution/dialysis method and a detergent binding method. In the dilution/dialysis method, the channel in 200 μL aliquots was mixed with detergent-solubilized asolectin, briefly sonicated, and then diluted 200-fold in PBS. This mixture was centrifuged at 100000*g* for 1 h, and the pellet resuspended in 1 mL of PBS and dialyzed overnight against 2 L of PBS. In the detergent binding method, the channel mixed with lipid was loaded into an Extracti-Gel D resin column (Pierce) and eluted with two column volumes of PBS. The reconstituted channel elutes in the void volume.

Electrophoresis and Immunoblotting. SDS−PAGE (*14*) was performed on 15% gels. Sample buffer was modified slightly by reducing the SDS to 0.25−0.5%. Samples were loaded without boiling unless specifically noted. Proteins

were transferred into polyvinylidene fluoride (PVDF) membranes (Bio-Rad) by electrotransfer according to the manufacturer's instructions. Membranes were blocked 1 h at room temperature in 5% nonfat milk in PBS, pH 7.4, and then incubated overnight in polyclonal anti-RGS-(4 × His) antibody (1:3000 dilution) at 4 °C. After two washes in PBS containing 0.05% Tween 20, the membranes were incubated with horseradish peroxidase-conjugated anti-mouse antibodies (1:5000 dilution) for 2 h. Bands were detected by chemiluminescence using ECL reagents and X-ray film.

Functional Assays

Oocyte Expression. Heterologous expression of SKC1 in *Xenopus* oocytes and electrophysiology were carried out essentially as described in Perozo et al. (*15*) with the following modifications: the SKC1-pQE32 cDNA was linearized with *Sal*I, and cRNA from was prepared with the Message Machine transcription kit (Ambion, Austin, TX) following the manufacturer's instructions. *Xenopus* oocytes at stages V and VI were injected with 50−60 nL of cRNA without dilution. Oocytes were maintained for several days in a saline solution (100 mM NaCl, 2 mM KCl, 1.8 mM $CaCl_2$, 1 mM $MgCl_2$, 5 mM HEPES-Na, pH 7.5, 2.5 mM pyruvate, and supplemented with 50 μg/mL gentamycin) at 18 °C.

Currents were recorded using the cut-open oocyte technique (*16*). Analog signals were filtered to 10 kHz, digitized at 50 ms/point, and stored in an IBM-compatible computer. The external and guard compartments were bathed in a solution containing 120 mM sodium methanesulfonate, 2.5 mM KCl, 1.8 mM $CaCl_2$, and 10 mM NMG-HEPES, pH 7.6. The internal compartment contained 110 potassium glutamate, 10 NMG-EGTA, and 10 NMG-HEPES, pH 7.6.

Tl^+ Quenching Experiments. We have used a simplified version of the fluorescence quenching method of Moore and Raftery (*17*) to qualitatively follow ion fluxes in proteoliposomes containing SKC1. This method is based on the selective permeability of a heavy metal ion into a lipid vesicle, quenching the fluorescence of an internalized fluorophore. This method, or variations of it, has been used successfully to measure ion fluxes in native membranes (*17*, *18*) and reconstituted systems (*19*,*20*). The approach we have followed is to determine whether or not reconstituted SKC1 is permeable to K^+ ions (or the K^+ analogue, Tl^+) at rest. To do so, we have monitored with low time resolution the quenching of an internally trapped fluorophore by external thallous ions.

Proteoliposomes containing reconstituted SKC1 channels were loaded by three cycles of freeze−thaw−sonication with 15 mM 1,3,6,8-pyrenetetrasulfonic acid (PTS, Molecular Probes, Junction City, OR) in a buffer with 100 mM $NaNO_3$ and 10 mM Tris-HCL, pH 7.5. The external PTS was subsequently removed by gel filtration over a Sephadex G-50 column. In a typical experiment, PTS-loaded vesicles were mixed 1:1 with a solution containing 100 mM $TlNO_3$ and 10 mM Tris-HCL, pH 7.5 (adjusted at the same osmolality of the internal solution). The mixing and simultaneous fluorescence measurement were performed on a Gilson SFM-25 fluorometer with a thermostated cell holder (at 20 °C) and vigorous stirring. The excitation and emission wavelengths were set to 355 and 404 nm, respectively.

Hydrodynamic Properties. The behavior of the SKC1 oligomer in detergent solution was analyzed by gel filtration chromatography. A sample (200 μL) of metal-chelate chromatography-purified SKC1 was applied on a Superose 200 column (1 × 30 cm). The column was pre-equilibrated with 1 mM DDM in PBS, pH 7.5. The flow rate was set to either 0.5 or 1 mL/min. Protein peaks were monitored by measuring the absorbance of the eluate at 280 nm in a Waters diode array detector, model 996. The column was calibrated with globular proteins of known Stokes radii under identical conditions as those used for SKC1. It must be pointed out, however, that the use of globular protein standards for the determination of the Stokes radius in membrane proteins tends to produce overestimated values (*21*). Accordingly, data must be interpreted with caution. The following proteins were used as standards (Stokes radii in parentheses): thyroglobulin (8.6 nm), ferritin (6.06 nm), alcohol dehydrogenase (4.6 nm), bovine serum albumin (3.55 nm), carbonic anhydrase (2.28 nm), and cytochrome *C* (1.65 nm). Column void volume (V_o) and total volume (V_T) were calibrated with dextran blue and potassium dichromate, respectively. For each protein, the distribution coefficient (K_D) was calculated according to the equation $K_D = (V_e - V_o)/(V_T - V_o)$, where V_e is the elution volume of each standard protein. The Stokes radius of the SKC1 mixed micelle was calculated from interpolation of the calibration curve.

Chemical Cross-Linking. Four homo-bifunctional cross-linkers with different arm spacings were used: disuccinimidyl tartarate, DST (6.4 Å); disuccinimidyl glutarate, DSG (7.7 Å); dimethylapidimate-2HCl, DMA (8.6 Å), and disuccinimidyl suberate DSS (11.4 Å) (all from Pierce). Samples (100 μL of 0.75 μM SKC1 in 1 mM DDM) were incubated in the presence of increasing concentrations of each of the cross-linking reagents for 3 h at room temperature. The reaction was stopped by addition of 20 mM Tris, pH 7.4, incubated for 15 min. Each sample was acetone precipitated, resuspended in sample buffer, and resolved by SDS−PAGE in a 15% gel. All samples were boiled, except for one unreacted control. Cross-linked proteins were transferred to PVDF and immunoblotted as described above.

Circular Dichroism Spectroscopy

CD Spectra were measured in a Jasco J720 spectropolarimeter (Jasco Inc., Tokyo, Japan) at room temperature. Spectra were obtained between 190 and 250 nm at a 1 nm interval in a 0.1 mm path length strain-free cylindrical cuvette (Hellma, Jamaica, NY) placed as close as possible to the photomultiplier. Samples in PBS were diluted 10-fold with 1 mM DDM in water, resulting in a final salt concentration of 14 mM. Typical protein concentration was between 2 and 5 μM. The average of 10−15 individual spectra was used for each sample. In all cases, the base line spectra used for subtraction were obtained from samples containing all components except the protein. Measured ellipticities, Θ, were converted to molar ellipticity, $[\Theta]$, by the relation

$$[\Theta] = (\mathrm{MRW} \times \Theta)/10lc$$

where MRW is the mean residue weight of SKC1 (111.4 g/mol), l is the path length (0.01 cm), and c is the protein concentration (mg/mL).

Quantification of secondary structures was carried out with the self-consistent method (*22*). We used a four basis spectra set (α-helix, β-sheet, β-turn, and random coil) derived from the high-resolution crystal structures of up to 14 proteins with secondary structure assignments according to the method of Kabsch and Sander (*23*). Molar ellipticity data corrected for background was analyzed using the program

Dicroprot (*24*). Protein concentration was determined from the absorbance at 280 nm and SKC1 molar extinction coefficient, calculated on the basis of its amino acid sequence (*25*).

Secondary Structure Prediction

The sequence from the histidine-tagged construct of SKC1 was analyzed by four independent methods: PHD, which is based on a two-layered feed-forward neural network using sequence alignment information and a non-redundant protein database (*26*,*27*); SOPMA, which is based on statistical comparisons of the test sequence with a database of non-homologous sequences (*28*); nn-predict, which uses a neural network to detect periodicities in the input sequence (Kneller et al., 1990); and Predator, which relies on local alignments of the query sequence with sequences in a non-homologous protein set (*29*). In all cases, the sequence (in FASTA format) was submitted to an automatic mail server for secondary structure prediction. Single-residue predictions for each method were aligned to SKC1 sequence, and a consensus secondary structure prediction was constructed on the basis of a per-residue average.

RESULTS

Oligomeric Behavior of SKC1

We have been able to express and purify, at milligram scale, the small K^+ channel from *S. lividans*, in agreement with previously reported data (*6*). Initial comparison of whole *E. coli* homogenates (boiling all samples prior to gel loading) identified an intense band that migrated at approximately 19 kDa, the predicted molecular weight of the hexahistidine-tagged SKC1 construct. Surprisingly, when samples were loaded without a boiling step, the protein migrated close to 65 kDa, suggesting that SKC1 is expressed in *E. coli* as an oligomer and that, remarkably, this oligomer is stable even in the presence of very harsh detergents like SDS. Direct size estimation of SKC1 homo-multimers predicts 39 kDa for a dimer, 58 kDa for a trimer, and 77 kDa for a tetramer, based on the hexahistidine-tagged construct size. Therefore, the 65 kDa oligomer could represent either a trimer or a tetramer migrating anomalously.

Figure 1 illustrates the general purification steps followed by SDS−PAGE. SKC1 targets to the membrane fraction (Figure 1, lane 3) and can be solubilized as oligomers using nonionic detergents (Figure 1, lane 4). The channel can be purified to homogeneity (Figure 1, lane 5) using metal-chelate chromatography followed by gel filtration chromatography on Superdex 200. Extensive boiling irreversibly disrupts the oligomeric association of SKC1 monomers, as shown in Figure 1A, lane 6, where a purified SKC1 sample (lane 5) was loaded into the gel after 2 min of boiling. When an identical experiment was analyzed by immunoblotting (Figure 1B), the oligomer/monomer migration pattern of SKC was revealed for all stages of the purification. Even when there is a single oligomer band in Coomassie-stained gels (Figure 1A, lane 5), Western blot analysis reveals the presence of low levels of monomer. We believe that the presence of small amounts of the monomer in these gels is due to a direct effect of SDS on oligomer stability and not to the presence of a small denatured fraction. Experiments with native gels, as well as the monodisperse behavior of the purified sample on gel filtration columns, tend to confirm this interpretation (see Figure 5).

In order to establish the best solubilization conditions in terms of extraction yield and stability, we have systematically

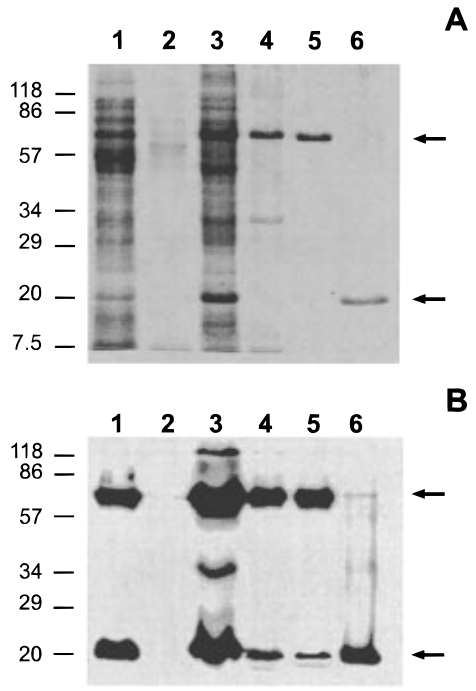

FIGURE 1: Oligomeric behavior of SKC in SDS−PAGE. SKC1 expressed in *E. coli* incorporates into the membrane and migrates primarily as either a 65 kDa oligomer or a 19 kDa monomer (arrows). (A) Coomassie-stained gel. (B) Western blot probed with the anti-RGS-(4 × His) anitibody. Left, molecular weight standards. Lane 1, IPTG-induced whole bacterial extract. Lane 2, supernatant. Lane 3, membrane fraction. Lane 4, membrane fraction solubilized with 16 mM dodecyl maltoside. Lane 5, purified SKC1. Lane 6, purified SKC1 after boiling 5 min. The black arrows point to the position of the monomer and oligomer bands.

tested an array of detergents by their ability to solubilize SKC1 in oligomeric form. Three types of detergents were tested: ionic (SDS, lauryl sarcosine), bile salts (DOC, CHAPS), and nonionic (Lubrol PX, Triton X-100, C8E4, Hega 10, Mega 9, OG, DDM, Fos-Choline, and Cymal 5). Aliquots of the spheroplast preparation were solubilized for 1 h with each of the detergents at ten times their CMC. Each sample was centrifuged 30 min at 100000*g*, and the supernatant was loaded on a gel containing 0.5% SDS. Sample buffer did not contain SDS. Proteins were transferred to PVDF membranes and blotted with anti-RGS-(4 × His) antibody, and bands were detected on X-ray film by chemiluminescence. The intensity of each band was measured after digitizing the X-ray film. The effectiveness of each detergent (in terms of yield) was determined by comparing the relative intensity of the oligomer band (Figure 2A).

It is clear that rigidly structured detergents (DOC, CHAPS) are not very effective in solubilizing SKC1. Unexpectedly, OG, a detergent widely used in the solubilization of integral membrane proteins, was the worst performer among nonionic detergents. When normalized by yield, most detergents are able to solubilize the channel while maintaining its oligomeric structure, as measured from the monomer/oligomer intensity ratio (Figure 2B). However, as expected, ionic detergents like SDS and lauryl sarcosine promoted oligomer dissociation. One surprise was Fos-Choline, the only nonionic detergent that induced partial oligomer dissociation. Remarkably, the purified channel is extremely stable in detergent solution. As assayed by SDS−PAGE under the conditions mentioned above, SKC1 maintains its oligomeric

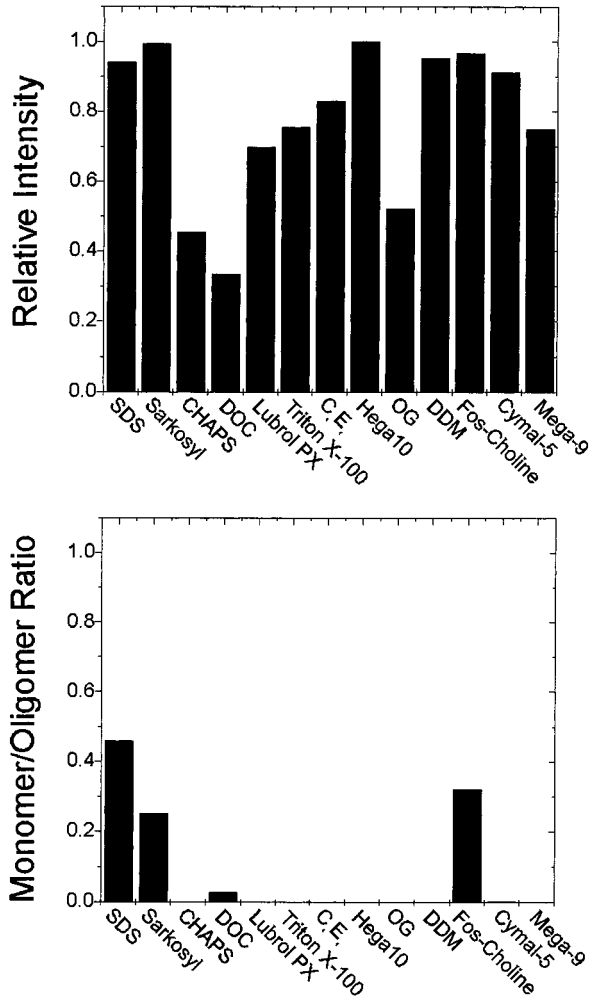

FIGURE 2: Detergent screening of SKC1 solubilization. Thirteen different detergents were compared according to their ability to solubilize SKC1 in the oligomeric state. (A) Optical density of the oligomeric band (65 kDa) quantified from densitometric scans of Western blot films for each of the tested detergents at 10× their CMC. Values are normalized against the highest intensity. (B) Comparison of the intensity ratio for the monomer and oligomer bands for each detergent.

structure in DDM at room temperature for more than a month (data not shown).

Because there was no *a priori* reason to expect a voltage or ligand-dependent gating mechanism in this channel, we anticipated that, at rest, SKC1 would mostly populate the open state. This condition would allow us to detect fluxes of K-channel-permeable ions (K^+, Tl^+, Rb^+) from reconstituted SKC1 channels. SKC1 was reconstituted into asolectin liposomes either by dilution/dialysis or by direct detergent absorption on hydrophobic beads (Reacti-D gels). Reconstituted channels were assayed by their ability to mediate Tl^+ fluxes in the presence of a trapped hydrophobic fluorophore (*17*). Figure 3 illustrates a typical experiment in which the fluorescence signal from vesicle-trapped PTS added into a buffer containing 150 mM Tl^+ is followed as a function of time. Under these conditions, a channel-specific Tl^+ flux can be detected as an instantaneous decrease in PTS fluorescence, given that the Tl^+ concentration inside the vesicles will probably equilibrate within 200 ms. Three different conditions were compared: pure asolectin vesicles (control), SKC1-containing proteoliposomes, and valinomycin-containing vesicles (positive control). The results in Figure 3 clearly indicate that reconstituted SKC1 is not able to mediate Tl^+ fluxes under these conditions. In control

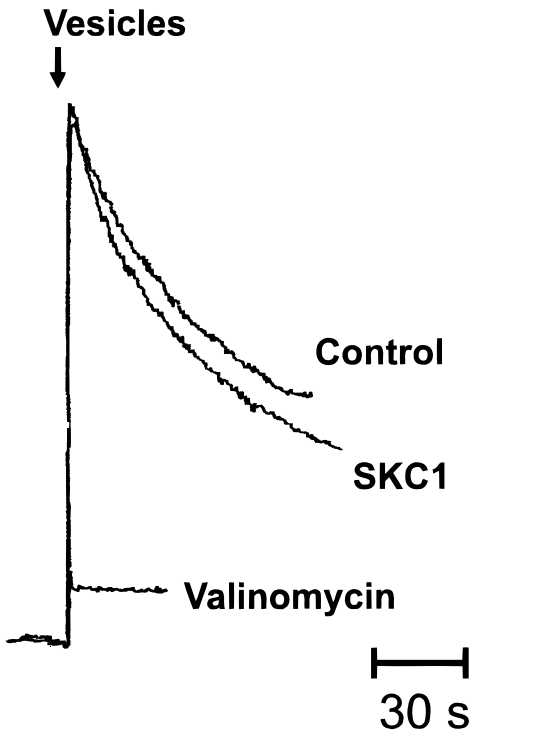

FIGURE 3: Thallous ion fluorescent quenching as a functional assay for SKC1. Vesicles containing 12 mM PMT were added, under constant stirring, into a buffer solution containing 200 mM $TlNO_3$. Three conditions were compared: control lipid vesicles, reconstituted SKC1 (60 μg of SKC1/mg of lipid), and lipid vesicles containing 1 μg/mL of valinomycin.

vesicles there is a slow yet measurable decrease in PTS fluorescence ($\tau = 23$ s), probably due to a direct permeability of neutral, undissociated $TlNO_3$ into the liposomes. SKC1-containing vesicles showed a slightly faster time course ($\tau = 20$ s), which is still too slow to be explained as a channel-mediated permeability. We tested several proteoliposome preparations with protein/lipid ratios between 10 μg/mg of lipid (~1:10000 molar ratio) and 60 μg/mg (~1:1500 molar ratio), with essentially identical results. When proteoliposomes containing SKC1 were solubilized in DDM and the protein was analyzed by SDS−PAGE, reconstituted SKC1 migrated at the same position as the 65 kDa band obtained from DDM-solubilized spheroplasts. We have taken this result as a direct indication of the oligomeric nature of the reconstituted channel, suggesting that the reconstitution process has not compromised the overall structure of channel.

In a second attempt to obtain functional information, we injected messenger RNA in *Xenopus* oocytes and the expression of SKC1 was followed by voltage clamp experiments using the cut-open oocyte technique (*16*). We were not able to detect any extra ionic currents due to the injection of SKC1 cRNA. Failure to detect currents occurred within a wide range of cRNA concentrations and even while incubating the injected oocytes for up to seven days (data not shown).

Thermal Stability of the SKC1 Oligomer

Given the remarkable stability of SKC1 oligomers in SDS micelles, we were interested in studying its thermal stability using SDS−PAGE as an assay for oligomeric structure. Identical aliquots of SKC1 in 1 mM DDM were incubated at different temperatures for 30 min and were then resolved on low concentration SDS gels and visualized by Coomassie staining. Figure 4A shows one such experiment. The

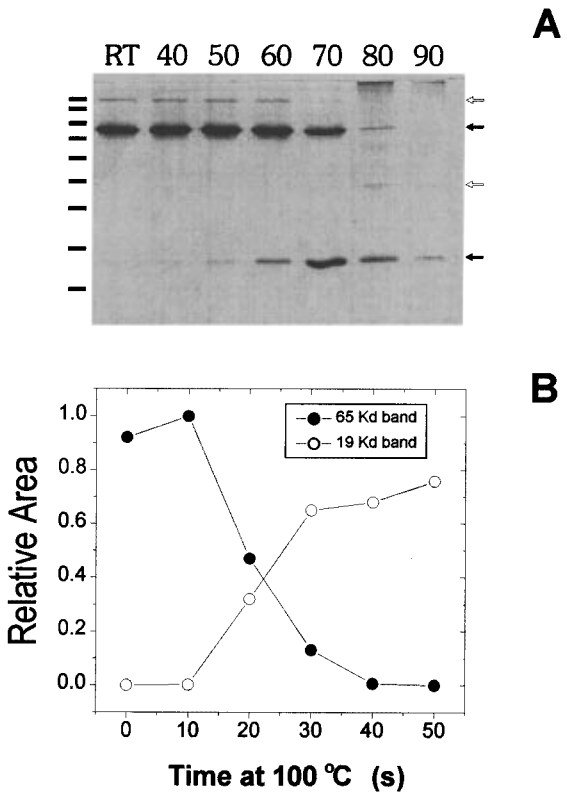

FIGURE 4: Thermal stability of SKC1. (A) Purified SKC1, solubilized in DDM, was incubated for 30 min at the indicated temperatures, electrophoresed on a 15% gel, and Coomassie stained. The black arrows point to the 65 and 19 kDa bands. The white arrow indicates the presence of higher molecular weight complex (a channel dimer). Molecular weight standards (from the top): 116, 97, 67, 55, 43, 36, 27, 20, and 14 kDa. (B) SKC in 1 mM DDM was incubated in boiling water for different amounts of time, and the intensity of the oligomer and monomer bands was quantified by desitometric scans of Western blot film.

oligomeric arrangement of SKC1 appears to be stable at temperatures up to 70 °C. Direct quantification of the monomer and oligomer bands was carried out by densitometric analysis of digitized gels, and the monomer/oligomer intensity ratio was used to obtain a thermal denaturation profile. Using this method, we determined that the oligomer-to-monomer transition occurs at temperatures between 58 and 83 °C, with a midpoint around 66 °C. An additional demonstration that the 65 and 19 kDa bands are directly related comes from experiments in which the thermal denaturation of the SKC1 oligomer was followed as a function of time, from measurements of the area-to-intensity product of both the monomer and oligomer bands (Figure 4B). Here it is clearly demonstrated that the fraction of oligomers that disappears at the oligomer band tends to appear as monomeric SKC1.

Hydrodynamic Behavior in Mixed Micelles

The dimensions of the SKC1 oligomeric complex have been deduced from the behavior of the mixed micelles in solution. Metal-chelate chromatography-purified SKC1 in 1 mM DDM was analyzed by gel filtration chromatography on a Superdex 200 column. The Stokes radius of the protein−detergent complex was determined from calibration plots based on the chromatographic separation of standard proteins of known radii (Figure 5A). Figure 5C shows that a plot of Stokes radii versus the elution parameter (K_{av}) is essentially linear for the standard proteins run on the Superdex 200 column. Interpolation of the elution parameter for SKC1 in the calibration curve described above yields a Stokes radius of 5.1 ± 0.3 nm. This value is consistent with a globular protein of about 120 kDa and confirms that, within the boundaries of a DDM micelle, SKC1 behaves like an oligomer. In Figure 5B, an identical SKC1 sample was boiled before it was resolved by gel filtration chromatography. This experiment shows that thermal disruption of the SKC1 oligomer completely alters its chromatographic profile, with a sharp decrease of the main oligomer peak, and the appearance of a long trailing peak of smaller molecular weight structures. The fact that a peak corresponding to the pure monomer is not observed is expected in the presence of nonionic detergent and suggests that SKC1 partially refolds at room temperature.

Stoichiometry of the Oligomeric Complex

In order to determine whether the SKC1 oligomer is either a trimer or a tetramer, we chemically cross-linked purified SKC1 solubilized in DDM. Four different homo-bifunctional cross-linking reagents, with primary amine specificity and different spacer arm length (in parenthesis), were used: DST (6.4 Å), DSG (7.7 Å), DMA (8.6 Å), and DSS (11.4 Å). Figure 6A shows an immunoblot in which identical samples of SKC1 solubilized in 1 mM DDM were cross-linked in the presence of increasing concentrations of DST and subjected to SDS−PAGE. In order to detect the degree of cross-linking, every sample, except for a control, was boiled before electrophoresis. At 1 mM DST, cross-linked SKC1 runs as a ladder of four bands, the largest of them coinciding with oligomeric SKC1 and the smallest with its monomeric form. Lower concentrations of DST reduce the intensity of the 65 kDa band, but the three other bands are still maintained. Figure 6B illustrates the linear relation that exists when the relative migration (R_f) of each of the cross-linked bands is plotted against the putative number of subunits they represent, assuming tetrameric stoichiometry. Interestingly, under the present experimental conditions only two of the reagents, DST and DSG, produced the characteristic four-band pattern of Figure 6A. DMA and DSS, which have spacer arms longer than 8 Å, failed to cross-link SKC1, a result which would suggest very specific limits for the overall backbone flexibility of this molecule.

We have found that SKC1 is particularly susceptible to proteolysis from intrinsic *E. coli* proteases. This can be observed by performing a standard purification from *E. coli* homogenates in the absence of protease inhibitors. Figure 7 (lane 2) shows one of these experiments. SDS−PAGE analysis of these samples shows a pattern of five bands running as an evenly spaced ladder, each differing in about 5 kDa from its larger neighbor and ranging from approximately 65 to 48 kDa. All of these bands are detected by immunoblotting with anti-RGS-(4 × His) antibody, which identifies them as SKC1 proteolytic products. Furthermore, because these proteins are recognized by its N-terminal epitope, the proteolytic site must be close to the C-terminus. It has not escaped our attention that this phenomenon can also be used to demonstrate the tetrameric nature of the SKC1 oligomeric complex. Thus, the simplest interpretation of the banding pattern observed in the absence of proteolytic inhibitors is that SKC1 is indeed a tetramer and each of the five bands represents this tetramer at different stages of proteolysis (see cartoon, Figure 7).

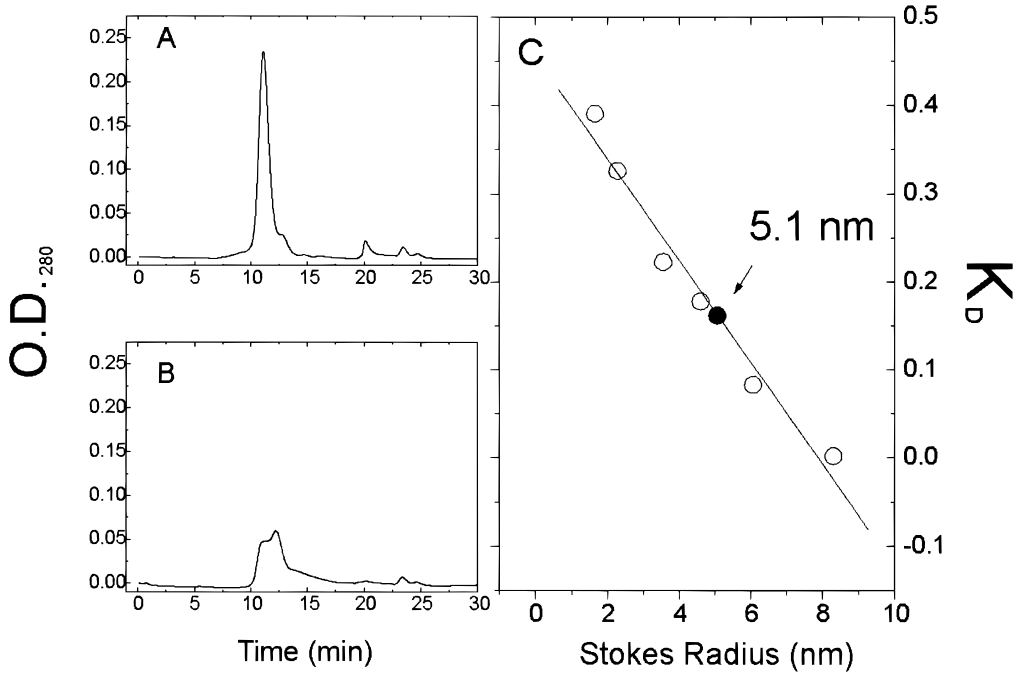

FIGURE 5: Gel filtration chromatography of DDM-solubilized SKC1 and estimation of Stokes radius of the mixed micelle. (A) Superdex 200 elution of a SKC1 preparation purified by metal-chelate chromatography. (B) Elution of the sample in A boiled for 2 min. (C) Estimation of the Stokes radius from linear interpolation of protein standards: thyroglobulin, ferritin, alcohol dehydrogenase, bovine serum albumin, carbonic anhydrase, and cytochrome *C*.

In certain gels, an intermediate 38 kDa band and a larger 120 kDa band can be observed (see Figure 1B, lane 3, and Figure 4). We have interpreted these bands as being stable complexes between two SKC1 monomers or two SKC1 tetramers, present at low abundance. The "half-channels" may actually establish similar helix−helix interactions as in the tetramer and could represent a stable intermediate in the process of SKC1 channel assembly. In our cross-linking experiments we did not detect any adducts larger than the 65 kDa band, which would suggest that the "channel dimers" represent a low-abundance configuration of SKC1.

Estimation of Secondary Structure

Figure 8 shows the CD spectra obtained from DDM-solubilized or asolectin-reconstituted SKC1. In both cases the spectra show a maximum around 193 nm and a broad negative peak with minima at 209 and 221 nm. These features are characteristic of proteins with a strong helical content. Close examination of the data reveals that both spectra are very similar down to about 200 nm. At lower wavelengths the spectra from reconstituted SKC1 diverges from the solubilized SKC1, suggesting a partial loss of helical structure upon reconstitution. We believe this effect to be an artifact of the measurement and not a real change in the secondary structure due to lipid insertion. Although efforts were made to minimize the light-scattering contribution from the liposomes, the decreased amplitude in ellipticity at lower wavelengths probably originates from differential light scattering and absorption flattening, typical of vesicular preparations larger than ~400 nm (*30*,*31*).

The secondary structure content of SKC1 was calculated using the self-consistent method (*22*) together with the secondary structure assignments of Kabsch and Sander (*23*). This analysis indicated that SKC1 is more than 50% α-helical, close to 20% β-sheet, 10% β-turn, and about 15% unassigned or disordered. There is, however, a 10% difference in the helical content obtained from the solubilized (59%) and reconstituted (50%) channels. As established above, the lower helical content of the reconstituted sample is most likely an underestimation due to liposome-derived light-scattering effects. The results of this analysis are summarized in Table 1.

As a comparison, the secondary structure of SKC1 based on its primary sequence was predicted by the use of four independent algorithms: PHD (*26*,*27*), SOPMA (*28*), nnpredict (*32*), and Predator (*29*). Only residues predicted to be α-helical or β-sheet structures were considered. These results were aligned, and a consensus secondary structure was assigned to each residue if at least 50% of the predictions agreed (Figure 9). All of the predictions point to a high helical content for SKC1, with strong helical assignments for the N-terminus, for most of the C-terminus and for the first of the two putative transmembrane segments. There are two small regions with high probability for a β-structure. One is located around and within the P-region, and the other one is located toward the N-terminus of the second of the predicted transmembrane segments. In order to make comparisons between experimentally determined and calculated secondary structure content, all of the predictions were performed on the His-tagged construct sequence. This construct contains 14 extra residues, which are predicted not to have any stable secondary structure. The overall secondary structure prediction for SKC1 was 58% α-helical, 13% β-sheet, and 29% of the residues were either random coil or unassigned structure. A summary of these results is shown in Table 2.

DISCUSSION

In order to understand the molecular basis of ion channel gating and selectivity, high-resolution structural information is absolutely required. However, application of standard structural approaches to these questions has been precluded due to the size and complexity of these channels as well as to the lack of a source for biochemical amounts of purified

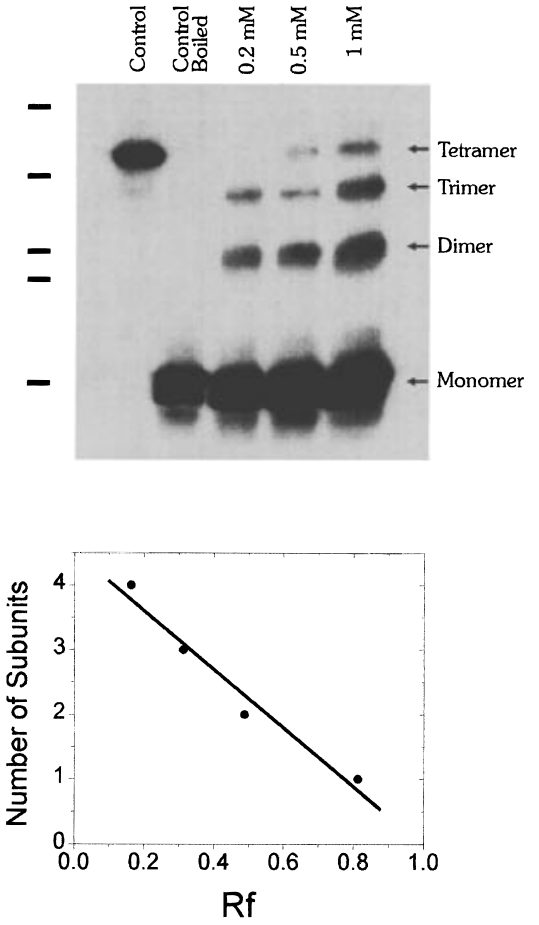

FIGURE 6: Chemical cross-linking of SKC1. (A) DDM-solubilized SKC1 was cross-linked with different concentrations of disuccinimidyl tartarate (DST) as described in Experimental Procedures. Each cross-linking reaction was resolved on 15% gels, transferred to a PVDF membrane, and detected by chemiluminescence. Since SKC1 runs as an oligomer under these conditions, all of the samples (except one of the controls) were extensively boiled prior to electrophoresis. In addition to the monomer, three bands are detected at higher molecular weights corresponding to the dimeric, trimeric, and tetrameric adducts of SKC1. (B) The apparent molecular weight of these bands shows a linear relation when the assumed number of subunits is plotted against the experimentally determined R_f values.

material. These problems are particularly relevant in the pursuit of structural information for voltage-dependent K^+ channels. The recent cloning and high-level expression of a K^+ selective channel from the gram-positive bacteria *S. lividans* (SKC1) (*6*) has opened the door to the application of multiple structural approaches to potassium selective channels.

Here, we have investigated the subunit stoichiometry and gross structural configuration of this channel as a prelude for high-resolution structural studies through the use of spectroscopic techniques. SKC1 was purified to homogeneity at multi-milligram levels as a fusion protein with a histidine tag. Initial electrophoretic analysis of this SKC1 construct indicated that the channel migrates mostly as a 65 kDa band, even in the presence of SDS. Furthermore, using gel shift as an assay for oligomeric thermal stability, we determined that the midpoint of the oligomer-to-monomer transition occurs at 65 °C. We were initially surprised with this behavior since most oligomeric complexes tend to dissociate under these conditions. However, oligomeric stability under harsh detergent or temperature conditions has been observed for the TM segments of other membrane

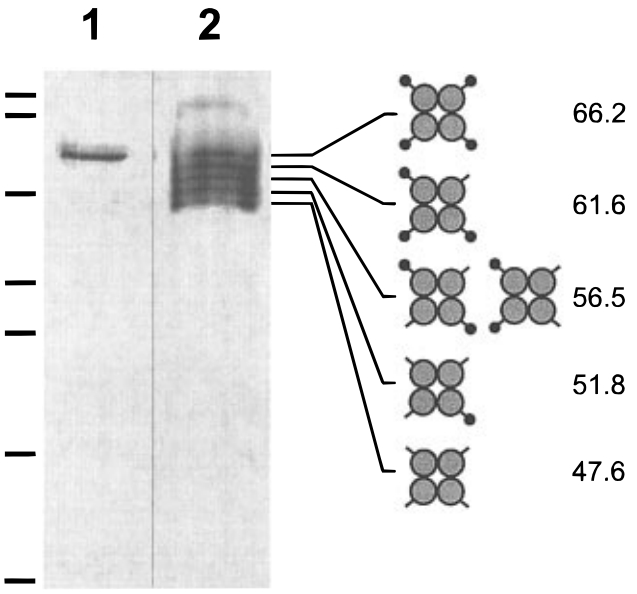

FIGURE 7: Proteolytic susceptibility of SKC1 also suggests a tetrameric arrangement. Lane 1, control SKC1 purified in the presence of protease inhibitors. Lane 2, SKC1 purified without protease inhibitors. A cartoon of a tetrameric channel at different stages of proteolysis represents each of the bands in the ladder. Left, molecular weight standards: 118, 86, 56.6, 34.1, 29, 19.6, and 7.5 kDa. The numbers indicate calculated molecular weights (in kDa) for each of the proteolysis intermediates.

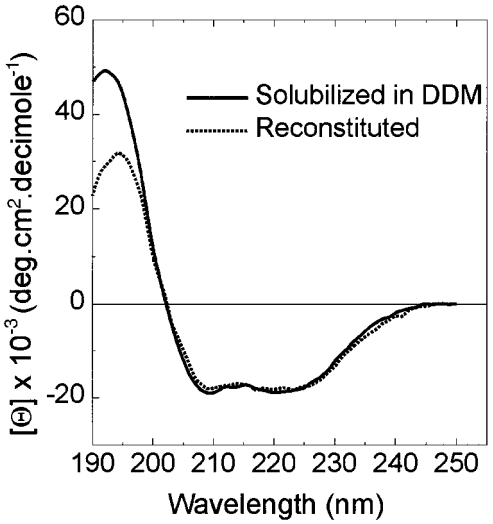

FIGURE 8: Circular dichroism spectra of SKC1. (—) SKC1 solubilized in 1 mM DDM. (···) SKC1 reconstituted into asolectin liposomes at a protein/lipid ratio of 1:500 (molar). Both spectra are averages of 10 individual scans and were obtained at room temperature.

Table 1: Secondary Structure Content in SKC1[a]

	SKC1 solubilized in DDM	reconstituted SKC1
α-helix	59.1 ± 0.8	50.8 ± 0.1
β-sheet	17.0 ± 4.2	19.5 ± 4.8
β-turn	8.3 ± 5.2	10.9 ± 7.1
other	15.9 ± 3.2	18.4 ± 4.7

[a] Values represent the mean ± standard deviation from at least three independent measurements.

proteins like glycophorin A (*33*) and phospholamban (*34*).

Glycophorin A, the major component of human erythrocyte membranes, forms dimers that are stable in SDS through very specific helix−helix contacts within the membrane-embedded region of the molecule. The two helices form a parallel right-handed helical supercoil (*35*) with van der

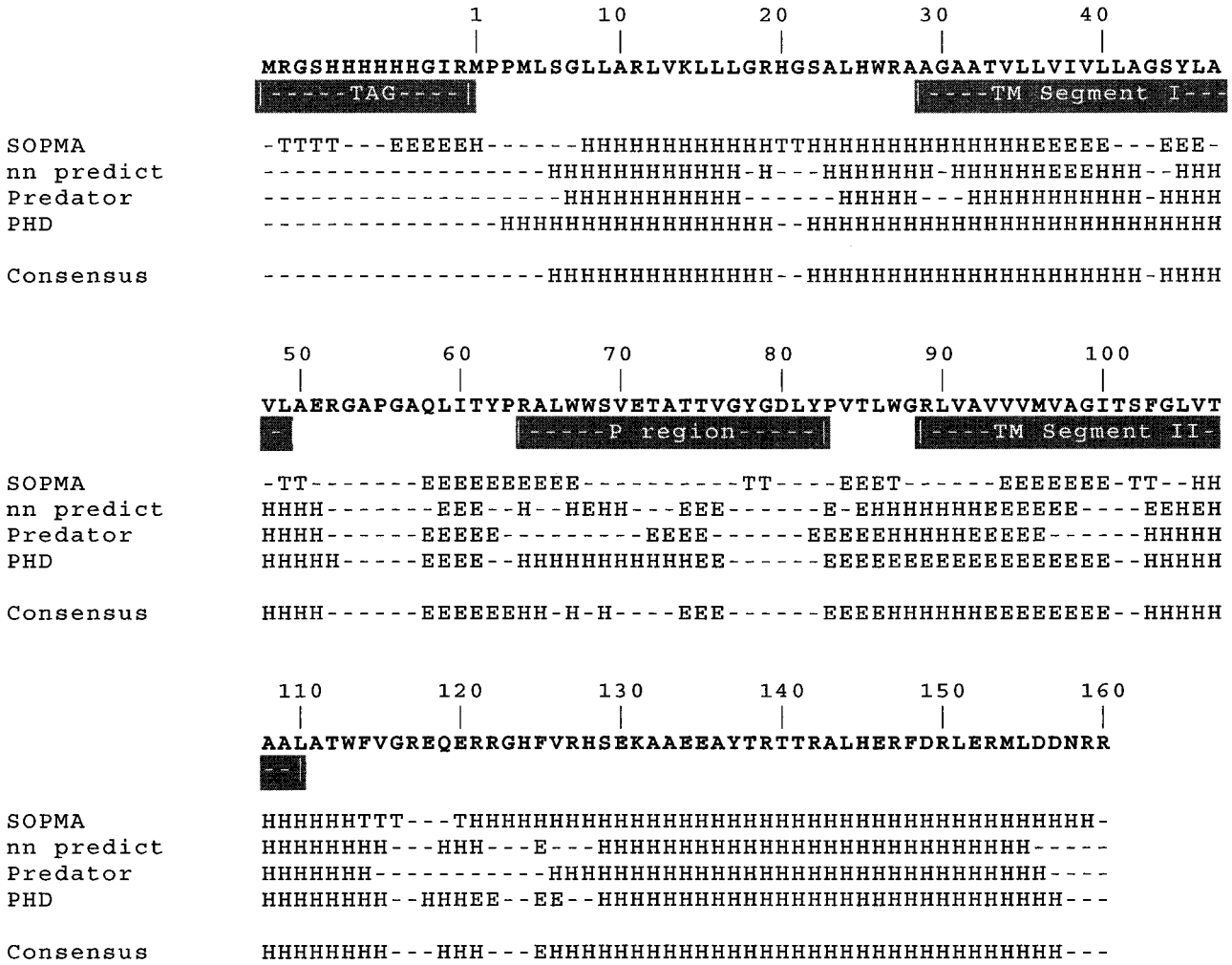

FIGURE 9: Secondary structure prediction of SKC1. Four independent algorithms were used to predict the secondary structure of SKC1 based solely on its primary sequence. The construct containing the Histidine tag and the RGS-(His × 4) epitope was used in all cases. Each prediction has been aligned to each other and to the amino acid sequence. A concensus per-residue prediction was obtained by averaging the four predictions at a given position. (H) α-helix, (E) *β*-sheet, (T) *β*-turn, (−) not assigned.

Table 2: Per-Residue Predicted Secondary Structures

structure	no. of residues	percentile
α-helix	101	58%
β-sheet	22	13%
N/A	50	29%

Waals interactions accounting for most of the stabilizing contacts (*36*). Phospholamban on the other hand, is a 52-amino acid regulator of the cardiac sarcoplasmic reticulum Ca^{2+} pump, contains a single TM segment, and associates as a pentamer (also stable in SDS). The phopholamban pentamer appears to be configured as a left-handed coiled-coil structure (*37*), and there is clear indication that a leucin heptad repeat is involved in helix−helix interactions (*38*). It is therefore tempting to suggest that a coiled-coil configuration could be responsible for the remarkable oligomeric stability of SKC1. According to the recent three-dimensional structure of glycophorin A (*36*), segments rich in *β*-carbon amino acids (V, I, T, L) are critical for dimer formation. Thus, according to these findings, the N-terminus of SKC1 and its first TM segment would be potential candidates for a coiled-coil structure.

That in fact the SKC1 oligomer is formed by the association of four identical subunits was shown on the basis of cross-linking experiments and partial internal proteolysis analysis. Considering that the monomer is 19 kDa, a Stokes radius of 5.1 nm, calculated from the hydrodynamic behavior of SKC1 in DDM micelles is also consistent with tetrameric stoichiometry for this channel. This homo-tetrameric configuration is a common structural arrangement among members of the voltage-dependent K^+ channel family that includes, true voltage-dependent channels with six transmembrane-segment subunits (*39*,*40*) as well as inward rectifier channels with two transmembrane-segment subunits (*41*,*42*).

A puzzling result of the present set of experiments has been our failure to demonstrate functional behavior in purified preparations of SKC1. Although Schrempf et al. (*6*) were able to measure and characterize SKC1 single-channel currents by either patch clamping of fused *Streptomyces* spheroplasts or measurements on artificial bilayers, a bulk functional assay of purified SKC1 has not yet been demonstrated. Using Tl^+ fluxes to quench the fluorescence of a trapped chromophore, we were unable to develop a "global" functional assay of reconstituted SKC1. Likewise, our attempts to use the *Xenopus* oocyte system to demonstrate macroscopic ionic currents in SKC1 were unsuccessful, in agreement with the original report (*6*). We can think of four possibilities to explain the absence of Tl^+ fluxes in the reconstituted preparation of SKC1: (1) the channel has been denatured or structurally compromised by purification; (2) it requires a specific lipid environment; (3) it is tightly gated by a still unknown mechanism; (4) it is missing a key structural or functional subunit. We believe that the first

possibility is unlikely. This is due to the fact that SKC1 forms stable tetramers and shows very specific nonrandom secondary structure (see below). Data supporting each of the remaining possibilities will have to be obtained empirically.

Far-UV circular dichroism spectroscopy is particularly sensitive to protein secondary structure and has been used extensively to estimate the relative content of secondary structure elements in proteins and peptides (*43*). Our preliminary estimation of SKC1 secondary structure content strongly indicates that the α-helix is the main structural element in this channel, both in detergent micelles and when incorporated into lipid membranes. There are, however, a number of methodological concerns related to the use of CD spectroscopy for secondary structure assignment in membrane proteins. At issue are the effects of light scattering and differential absorption (*31*,*44*), the use of basis spectra relevant to membrane proteins (*30*,*45*,*46*), and the known uncertainties in protein concentration determination (*47*). Therefore, the present data should be taken as preliminary estimations of secondary structure. A more precise picture of SKC1 sary structure assignments will come from CD data extended beyond 190 nm and from data obtained with complementary methods like Fourier transform infrared spectroscopy.

Nonetheless, these data tend to confirm the notion that SKC1 and, by extension, other members of the voltage-dependent K^+ family are held together as a bundle of helices, as suggested by previous topological models and recent experimental determinations of transmembrane topology (*48*,*49*). Still, the fact that nearly 20% of SKC1 appears to be in a β-extended configuration should be taken into consideration when structural models of this channel are formulated. It is interesting to note that our experimentally determined secondary structure agrees remarkably well with predictions based strictly on theoretical considerations, even in the absence of additional information derived from sequence alignments. This agreement should be taken as an independent validation of the present data and as an indication that SKC1 is expressed and purified in its native conformation.

ACKNOWLEDGMENT

The authors thank Drs. Michael Wiener, Robert Nakamoto, and Ruth Murrell-Lagnado for critically reading the manuscript and Drs. Christopher Miller, Lise Heginbotham, and Roderick MacKinnon for illuminating discussions. Dr. Fred Richardson and R. MacKinnon kindly provided access to CD spectropolarimeters.

REFERENCES

1. Jan, L. Y., and Jan, Y. N. (1992) *Cell 69*, 715−718.
2. Catterall, W. A. (1991) *Science 253*, 1499−1500.
3. Miller, C. (1991) *Science 252*, 1092−1096.
4. Jan, L. Y., and Jan, Y. N. (1994) *Nature 371*, 119−122.
5. Bezanilla, F., and Stefani, E. (1994) *Annu. Rev. Biophys. Biomol. Struct. 23*, 819−846.
6. Schrempf, H., Schmidt, O., Kummerlen, R., Hinnah, S., Muller, D., Betzler, M., Steinkamp, T., and Wagner, R. (1995) *EMBO J. 14*, 5170−5178.
7. Heginbotham, L., Abramson, T., and MacKinnon, R. (1992) *Science 258*, 1152−1155.
8. Milkman, R. (1994) *Proc. Natl. Acad. Sci. U.S.A. 91*, 3510−3514.
9. Pigac, P., Hranueli, D., Smokvina, T., and Alacevic, M. (1982) *Appl. Environ. Microbiol. 44*, 1178−1186.
10. Hopwood, D. A., Bibb, M. J., Chater, K. F., Kieser, T., Burton, C. J., M., K. H., Lydiate, D. J., Smith, C. P., Ward, J. M., and Schrempf, H. (1985) *Genetic Manipulation of Streptomyces. A Laboratory Manual*, The John Innes Foundation, Norwich, U.K.
11. Kaback, H. R. (1974) *Methods Enzymol. 31*, 698−709.
12. Bradford, M. M. (1976) *Anal. Biochem. 72*, 248−254.
13. Kagawa, Y., Kandrach, A., and Racker, E. (1973) *J. Biol. Chem. 248*, 676−684.
14. Laemmli, U. K. (1970) *Nature 227*, 680−685.
15. Perozo, E., MacKinnon, R., Bezanilla, F., and Stefani, E. (1993) *Neuron 11*, 353−358.
16. Taglialatela, M., and Stefani, E. (1993) *Proc. Natl. Acad. Sci. U.S.A. 90*, 4758−4762.
17. Moore, H. P., and Raftery, M. A. (1980) *Proc. Natl. Acad. Scie. U.S.A. 77*, 4509−4513.
18. Garcia, A. M., and Miller, C. (1984) *J. Gen. Physiol. 83*, 819−839.
19. Wu, W. C., Moore, H. P., and Raftery, M. A. (1981) *Proc. Natl. Acad. Sci. U. S.A. 78*, 775−779.
20. Tomiko, S. A., Rosenberg, R. L., Emerick, M. C., and Agnew, W. S. (1986) *Biochemistry 25*, 2162−2174.
21. Le Maire, M., Aggerbeck, L. P., Monteilhet, C., Andersen, J. P., and Moller, J. V. (1986) *Anal. Biochem. 154*, 525−535.
22. Sreerama, N., and Woody, R. W. (1993) *Anal. Biochem. 209*, 32−44.
23. Kabsch, W., and Sander, C. (1983) *Biopolymers 22*, 2577−2637.
24. Deleage, G., and Geourjon, C. (1993) *Comput. Appl. Biosci. 9*, 197−199.
25. Gill, S. C., and von Hippel, P. H. (1989) *Anal. Biochem. 182*, 319−326.
26. Rost, B., and Sander, C. (1993) *J. Mol. Biol. 232*, 584−599.
27. Rost, B., and Sander, C. (1994) *Proteins 19*, 55−72.
28. Geourjon, C., and Deleage, G. (1995) *Comput. Appl. Biosci. 11*, 681−684.
29. Frishman, D., and Argos, P. (1996) *Protein Eng. 9*, 133−142.
30. Park, K., Perczel, A., and Fasman, G. D. (1992) *Protein Sci. 1*, 1032−1049.
31. Mao, D., and Wallace, B. A. (1984) *Biochemistry 23*, 2667−2673.
32. Kneller, D. G., Cohen, F. E., and Langridge, R. (1990) *J. Mol. Biol. 214*, 171−182.
33. Furthmayr, H., and Marchesi, V. T. (1976) *Biochemistry 15*, 1137−1144.
34. Imagawa, T., Watanabe, T., and Nakamura, T. (1986) *J. Biochem. 99*, 41−53.
35. Lemmon, M. A., Flanagan, J. M., Treutlein, H. R., Zhang, J., and Engelman, D. M. (1992) *Biochemistry 31*, 12719−12725.
36. MacKenzie, K. R., Prestegard, J. H., and Engelman, D. M. (1997) *Science 276*, 131−133.
37. Arkin, I. T., Adams, P. D., MacKenzie, K. R., Lemmon, M. A., Brunger, A. T., and Engelman, D. M. (1994) *EMBO J. 13*, 4757−4764.
38. Simmerman, H. K., Kobayashi, Y. M., Autry, J. M., and Jones, L. R. (1996) *J. Biol. Chem. 271*, 5941−5946.
39. Schulteis, C. T., Nagaya, N., and Papazian, D. M. (1996) *Biochemistry 35*, 12133−12140.
40. MacKinnon, R. (1991) *Nature 350*, 232−235.
41. Yang, J., Jan, Y. N., and Jan, L. Y. (1995) *Neuron 15*, 1441−1447.
42. Silverman, S. K., Lester, H. A., and Dougherty, D. A. (1996) *J. Biol. Chem. 271*, 30524−30528.
43. Woody, R. W. (1995) *Methods Enzymol. 246*, 34−71.
44. Wallace, B. A., and Mao, D. (1984) *Anal. Biochem. 142*, 317−328.
45. Van Hoek, A. N., Wiener, M., Bicknese, S., Miercke, L., Biwersi, J., and Verkman, A. S. (1993) *Biochemistry 32*, 11847−11856.
46. Fu, D. X., and Maloney, P. C. (1997) *J. Biol. Chem. 272*, 2129−2135.
47. Johnson, W. C., Jr. (1990) *Proteins 7*, 205−214.
48. Shih, T. M., and Goldin, A. L. (1997) *J. Cell Biol. 136*, 1037−1045.
49. Johansson, M., and von Heijne, G. (1996) *J. Biol. Chem. 271*, 25912−25915.

BI971018Y